RITG148+

PERFORM COMPREHENSIVE QA FOR HELICAL TOMOTHERAPY WITH RIT

RITG148+ is a precise and state-of-the-art software built to perform all machine and imaging QA measurements for TomoTherapy® and Radixact® treatment delivery systems.

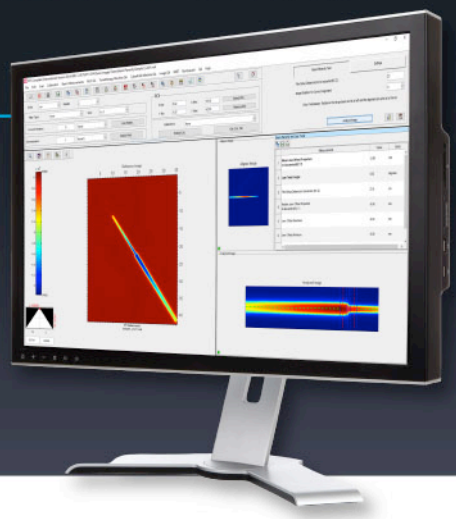

RIT offers two software packages for comprehensive daily, monthly, and annual TG-148 QA of helical tomotherapy machines. **RITG148+** includes analyses for Static & Rotational Output Consistency, Jaw Centering & Alignment, Overhead Laser Positioning, Interrupted Treatment, and more, as well as image quality analysis using the TomoTherapy cheese phantom. In addition to these tests, **RIT *Complete*** adds patient QA capabilities by providing an advanced TomoTherapy Registration feature.

AUTOMATED MACHINE QA TESTS

- Y-jaw/gantry rotation plane alignment
- Y-jaw divergence/beam centering
- Couch translation/gantry rotation
- Gantry angle consistency
- Treatment field centering
- Interrupted treatment
- MLC alignment test
- Laser localization

IMAGE QUALITY TESTS

- Noise
- Contrast
- Resolution
- Uniformity
- Geometric Accuracy
- Geometric Distortion
- CT Number to Density
- Crop images with the Pin Prick, Erase, and ROI tool

BUILT-IN FEATURES

RIT*trend*™ reporting and trending statistical database

PDF report exports for every analysis routine

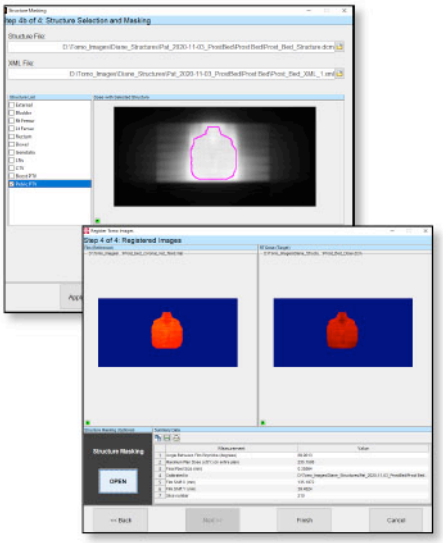

TOMOTHERAPY REGISTRATION WITH RIT *Complete*

Upgrade to RIT *Complete* to perform TomoTherapy® patient QA, in addition to all the machine and imaging QA tests in RITG148+. Easily perform exact dose comparisons using a TomoTherapy® plan, a dose map, and a film to determine position and dose accuracy using the red or green lasers, analyzing coronal or sagittal slices. RIT's analysis allows any structure in the Accuray Precision® plan (e.g. PTV) to display as an overlay ROI. Then, use RIT's Patient QA routines to measure your results (Gamma, Subtraction, DTA, or one of 34 other analysis routines) within the ROI.

RIT software's combination of innovative, robust routines with a user-friendly interface work together to maximize the efficiency and precision of your measurements.

SCHEDULE A PERSONAL DEMO OF RIT'S TG-148 CAPABILITIES TODAY!

RADIMAGE.COM®

+1.719.590.1077, Opt. 4 | sales@radimage.com | Connect with us on social media @RIT4QA

Received: 25 January 2022 | Revised: 18 April 2022 | Accepted: 23 May 2022

DOI: 10.1002/mp.15782

RESEARCH ARTICLE

MEDICAL PHYSICS

Application of a novel diamond detector for commissioning of FLASH radiotherapy electron beams

Gianluca Verona Rinati[1] | **Giuseppe Felici**[2] | **Federica Galante**[2] | **Alessia Gasparini**[3,4] | **Rafael Kranzer**[5,6] | **Giulia Mariani**[2] | **Matteo Pacitti**[2] | **Giuseppe Prestopino**[1] | **Andreas Schüller**[7] | **Verdi Vanreusel**[3,4] | **Dirk Verellen**[3,4] | **Claudio Verona**[1] | **Marco Marinelli**[1]

[1]Department of Industrial Engineering, University of Rome Tor Vergata, Rome, Italy

[2]SIT S.p.A., Latina, Italy

[3]Iridium Kankernetwerk, Antwerp, Belgium

[4]Faculty of Medicine and Health Sciences, Antwerp University, Antwerp, Belgium

[5]PTW-Freiburg, Freiburg im Breisgau, Germany

[6]University Clinic for Medical Radiation Physics, Medical Campus Pius Hospital, Carl von Ossietzky University, Oldenburg, Germany

[7]Physikalisch-Technische Bundesanstalt (PTB), Braunschweig, Germany

Correspondence
Marco Marinelli, Department of Industrial Engineering, University of Rome "Tor Vergata", Via del Politecnico, 1, 00133 Rome, Italy.
Email: marco.marinelli@uniroma2.it

Funding information
European Metrology Programme for Innovation and Research

Abstract

Purpose: A diamond detector prototype was recently proposed by Marinelli et al. (Medical Physics 2022, https://doi.org/10.1002/mp.15473) for applications in ultrahigh-dose-per-pulse (UH-DPP) and ultrahigh-dose-rate (UH-DR) beams, as used in FLASH radiotherapy (FLASH-RT). In the present study, such so-called flashDiamond (fD) was investigated from the dosimetric point of view, under pulsed electron beam irradiation. It was then used for the commissioning of an ElectronFlash linac (SIT S.p.A., Italy) both in conventional and UH-DPP modalities.

Methods: Detector calibration was performed in reference conditions, under ^{60}Co and electron beam irradiation. Its response linearity was investigated in UH-DPP conditions. For this purpose, the DPP was varied in the 1.2–11.9 Gy range, by changing either the beam applicator or the pulse duration from 1 to 4 μs. Dosimetric validation of the fD detector prototype was then performed in conventional modality, by measuring percentage depth dose (PDD) curves, beam profiles, and output factors (OFs). All such measurements were carried out in a motorized water phantom. The obtained results were compared with the ones from commercially available dosimeters, namely, a microDiamond, an Advanced Markus ionization chamber, a silicon diode detector, and EBT-XD GAFchromic films. Finally, the fD detector was used to fully characterize the 7 and 9 MeV UH-DPP electron beams delivered by the ElectronFlash linac. In particular, PDDs, beam profiles, and OFs were measured, for both energies and all the applicators, and compared with the ones from EBT-XD films irradiated in the same experimental conditions.

Results: The fD calibration coefficient resulted to be independent from the investigated beam qualities. The detector response was found to be linear in the whole investigated DPP range. A very good agreement was observed among PDDs, beam profiles, and OFs measured by the fD prototype and reference detectors, both in conventional and UH-DPP irradiation modalities.

Conclusions: The fD detector prototype was validated from the dosimetric point of view against several commercial dosimeters in conventional beams. It was proved to be suitable in UH-DPP and UH-DR conditions, for which no other commercial real-time active detector is available to date. It was shown to be a very useful tool to perform fast and reproducible beam characterizations

in standard clinical motorized water phantom setups. All of the previously mentioned demonstrate the suitability of the proposed detector for the commissioning of UH-DR linac beams for preclinical FLASH-RT applications.

KEYWORDS
diamond detector, dosimetry, FLASH radiotherapy

1 | INTRODUCTION

Since the discovery of the so-called FLASH effect in radiation therapy,[1] an increasing effort has been devoted to its study by many research groups all over the world.[2–12] The growing interest in FLASH radiotherapy (FLASH-RT) has driven a technological breakthrough leading to innovative accelerator facilities, capable of producing high- and ultrahigh-dose-rate (UH-DR) as well as high- and ultrahigh-dose-per-pulse (UH-DPP) beams.[13–19] This poses challenging requirements to the dosimetry of the radiotherapy beams generated by such a new class of accelerators.[8,9,20,21] Passive dosimeters, such as alanine[22–26] and GAFchromic films,[16,17,26–28] have been shown to be suitable for these purposes, with some limitations. In particular, their response can be obtained hours or even days later than the irradiation procedure, rendering the use of such detectors for the daily linac quality assurance tests requested for preclinical studies very impractical. Moreover, when using UH-DPP beams, the irradiation of GAFchromic films must be limited to a few pulses or even one single pulse to sit in their optimal detection window.[8,25,27] This results in an additional uncertainty in the dose rate determination due to possible fluctuations of the accelerator output. On the other hand, no commercial real-time response dosimetric systems are available yet for UH-DPP applications, due to recombination, saturation, and nonlinearity effects typically observed in the response of ionization chamber (IC)[15,24,26,28–31] and solid-state detectors such as silicon and diamond-based diodes.[8,15,20,31] Novel detector prototypes are being designed and characterized by several research groups,[30–32] whose properties are expected to overcome these limitations. In particular, a diamond Schottky diode detector prototype was recently proposed,[33] the so-called flashDiamond (fD), specifically designed for UH-DPP and UH-DR applications. A thorough characterization was performed in terms of detector response linearity, which has been proven for DPPs up to at least 20 Gy, average DRs of the order of 1 kGy/s, and instantaneous DRs of about 5 MGy/s. The fulfillment of this response linearity prerequisite demonstrated the feasibility of a diamond-based detector for FLASH-RT applications.

The present work is a step forward in view of the application of the fD detector in clinical studies. Two main aspects are addressed both in conventional and UH-DR irradiation conditions: (i) a comprehensive dosimetric validation of such detector and (ii) the application to the commissioning of an ElectronFlash linac (SIT S.p.A., Italy).

2 | MATERIALS AND METHODS

2.1 | Irradiation device

All the irradiation experiments reported in this study were performed by using an ElectronFlash linac (SIT S.p.A., Italy).[15,18] The main features of the accelerator are reported in Table 1. In particular, it can be operated both in conventional and UH-DPP modalities. Pulsed electron beams with two different energies are available (7 and 9 MeV). The pulse duration can be varied in the range of 0.5–4 μs. The pulse repetition frequency (PRF) can be varied as well, ranging from single pulse mode up to a maximum frequency of 245 or 500 Hz, for pulse durations of 4 and 2.5 μs, respectively. The linac is equipped with several polymethylmethacrylate (PMMA) cylindrical applicators, differing both in length and diameter. More specifically, applicators 30, 35, 40, 50, 100, and 120 mm in diameter were used in this study. It is worth mentioning that the length of the applicators varies as well, thus changing the minimum source-to-surface distance achievable by each applicator. This implies that different DPP ranges are obtained depending on the applicator used during the irradiation procedure. In our study, maximum DPPs of about 180 mGy and 11.9 Gy were achieved in conventional and UH-DPP modalities,

TABLE 1 Main features of the ElectronFlash linac used in this study

Parameter		Range		
Beam energy		**7 and 9 MeV**		
Pulse duration		**from 0.5 to 4.0 μs**		
Pulse repetition frequency		**from single pulse to 500 Hz**		
Applicators (mm)	**Ext. ∅ (mm)**	**Int. ∅ (mm)**	**SSD[a] (cm)**	**DPP_{max} (Gy)**
30	40	30	71.8	11.4
35	40	36	71.8	11.9
40	50	40	78.6	10.6
50	60	50	81.8	9.2
100	110	100	109.8	4.1
120	134	124	126.8	2.7

Note: The DPP_{max} values were obtained by EBT-XD films, positioned at d_{max}, under 9 MeV irradiation, with the phantom in close contact with the applicator.
[a]Source-to-surface distance.

respectively, by using 9 MeV electron beams and the 35 mm applicator. The ElectronFlash linac is equipped with an online monitoring system as per IEC-60601-2-1 prescription.[34] The beam is monitored by means of transmission detectors, that is, monitor chambers in conventional mode and current transformers in UH-DPP mode.[15,18]

2.2 | Dosimetric systems

In this study, an fD prototype was investigated, whose physical properties were recently reported by Marinelli et al.[33] It consists of a diamond Schottky diode, based on the same working principle of the commercially available PTW microDiamond (mD) (PTW-Freiburg, Germany).[35,36] The fD design and layout were specifically modified in order to meet the stringent requirements of UH-DPP applications. Its sensitive volume is a high purity intrinsic diamond, 1.4 mm in diameter and about 1 μm thick. The device housing is the same as used for the mD detector, so that the measuring point is located at 1 mm water equivalent depth below the housing top surface. Just as the mD detector, no external bias voltage is required for the fD operation, and a pre-irradiation of 5 Gy is recommended before daily use in order to get a stable response within 0.5%.

The response of the fD detector obtained in conventional and UH-DPP modalities was compared for validation with the ones of several well-assessed detectors. The latter were only used in the specific irradiation conditions in which they can be considered reference detectors. In particular, an Advanced Markus chamber (type 34045, PTW-Freiburg, Germany), a silicon diode (SiD) (type T60017, PTW-Freiburg, Germany), an mD detector (type 60019, PTW-Freiburg, Germany), and EBT-XD GAFchromic films (Ashland Inc., Bridgewater, NJ, USA) were used in conventional irradiation modality, whereas EBT-XD films only were used for comparisons in UH-DPP conditions. They were calibrated and analyzed by the FilmQA Pro software (Ashland Inc., Covington, KY, USA), according to the protocol suggested by the manufacturer and the measurement procedure reported by the authors in Ref. [33]. PTW electrometers were used for the measurements performed by active real-time detectors. In particular, a PTW UNIDOS E electrometer was used for all "static" measurements, such as absolute dose determinations, linearity tests, and output factors (OFs). As for percentage depth dose (PDD) and profile measurements, a PTW Tandem electrometer (PTW-Freiburg, Germany) was used, in combination with a motorized water phantom and the PTW Mephysto MC^2 software. It is worth mentioning that during the tests performed in UH-DPP irradiation conditions a 100 nF capacitance box provided by PTW was inserted in the readout chain, between the detector output and the electrometer input.[33] This is mandatory in order to limit the instantaneous current flowing through the electrometer below the threshold value reported in both the UNIDOS E and Tandem manufacturer specifications.

2.3 | Experiments

The absorbed dose calibration of the fD was performed in ^{60}Co irradiation at the PTW secondary standard laboratory, and under UH-DPP reference electron beams at the Physikalisch-Technische Bundesanstalt (PTB). In addition, it was cross-calibrated at SIT by comparison with an Advanced Markus IC, under irradiation by ElectronFlash beams in conventional modality and reference conditions (100 mm applicator at the point of maximum dose d_{max}).

Absolute dose measurements, linearity tests, PDDs, beam profiles, and OF measurements were then performed both in conventional and UH-DPP irradiation conditions, by using 7 and 9 MeV electron beam energies. Such measurements were carried out in a water phantom for all the detectors, with the only exception of EBT-XD films, in which case a PMMA phantom was used instead.

Response linearity tests were performed in UH-DPP modality with the 9 MeV electron beam energy, in two different irradiation conditions. In the first case, the DPP was varied by changing the PMMA applicators and positioning the water phantom entrance window in close contact with the applicator. The second measurement was performed in reference conditions, again with 9 MeV electrons. The DPP was varied by changing the beam pulse duration from 1 up to 4 μs. An overall range from about 1.2 up to 11.9 Gy/pulse was achieved by the combination of the two setups. In all cases, the fD detector positioning was carefully verified by measuring in-plane and cross-plane beam profiles. Its response, measured at the central beam axis and d_{max}, was compared with the one from EBT-XD films. They were irradiated, while sandwiched between PMMA slabs, whose thickness was properly chosen to obtain the same water equivalent depths as compared to the ones used for the fD detector.

PDD measurements were performed in conventional and UH-DPP conditions, both for 7 and 9 MeV beams, by using all the available PMMA applicators. The following parameters were used: 25 Hz PRF, 4 μs beam pulse duration, and 1 s Tandem electrometer acquisition time at each depth. A PTW semiflex IC (type 31010, PTW-Freiburg, Germany) was used as an out-of-field reference during the PDD acquisition, positioned outside the beam collimator where the beam intensity was low enough to prevent its response saturation. In order to evaluate uncertainty on the detector positioning, four sets of three PDDs each were recorded in the very same irradiation conditions, by removing and repositioning four times the fD detector in the water phantom. The standard deviation of the obtained R_{50} values was found

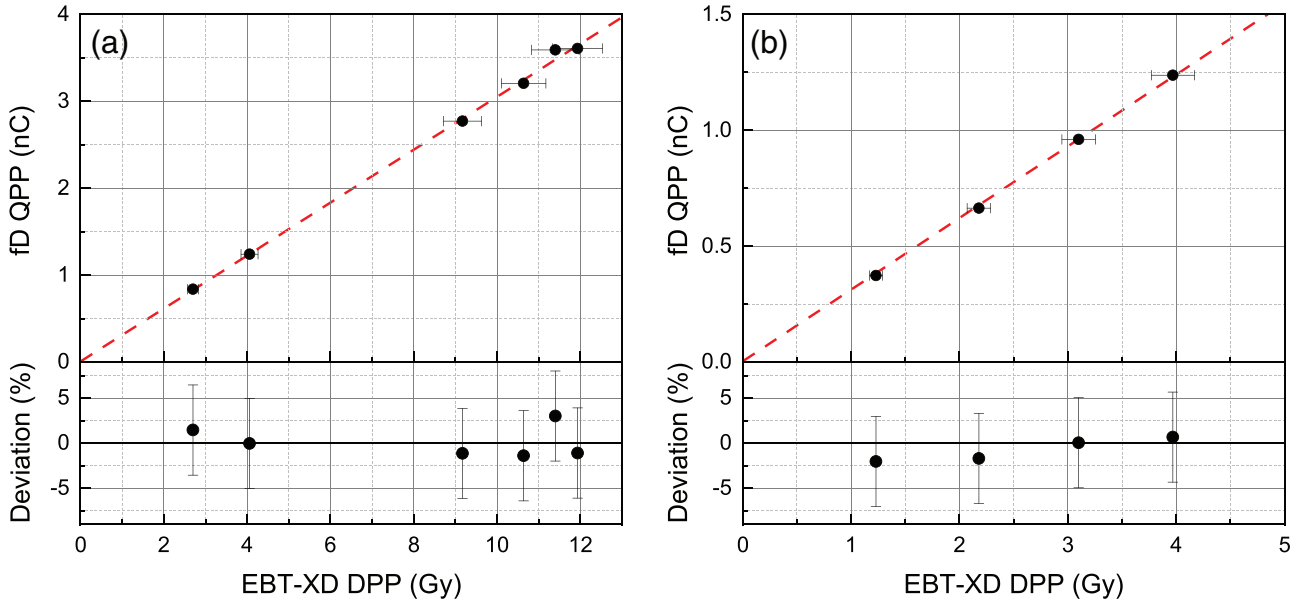

FIGURE 1 Charge per pulse (QPP) of the flashDiamond (fD) detector as a function of the dose-per-pulse (DPP) measured by EBT-XD films. The DPP was varied by changing the PMMA applicator (a) and the pulse duration (b). The red dashed lines are the linear best fits to the experimental data. Deviations from linearity plots are also reported in both cases.

to be 0.3 mm. Besides the fD detector, all the previously listed commercial detectors were used for comparing PDDs measured in conventional modality, whereas only EBT-XD films were used as reference in UH-DPP conditions. As for the GAFchromic film irradiation during PDD measurements, they were positioned parallel to the electron beam axis and sandwiched between PMMA slabs.

Beam profile measurements were performed by using the same irradiation conditions and acquisition parameters adopted for PDDs. They were recorded at d_{max}, as derived for each collimator from the previously measured PDD curves.

OFs were measured by the fD detector prototype in conventional and UH-DPP conditions as well, both for 7 and 9 MeV beams, by using all the available PMMA applicators. All the measurements were performed at d_{max}. One hundred fifty pulses at a PRF of 25 Hz were delivered for each OF measurement in conventional modality, whereas 25 pulses at 5 Hz were used in the case of UH-DPP irradiation conditions. The obtained results were compared with the ones from the SiD detector and EBT-XD films in the case of conventional and UH-DPP conditions, respectively. It is worth to point out that similar irradiation parameters could be used for the fD and SiD, whereas a much lower number of total pulses (from 1 to 10 depending on the actual DPP value) were delivered to GAFchromic films in order to prevent their response saturation.

3 | RESULTS

The fD prototype sensitivities obtained from the calibration procedures performed at PTB (UH-DPP electron beams), SIT (electron beams in conventional modality), and PTW (^{60}Co irradiation) are 0.305 ± 0.002, 0.306 ± 0.005, and 0.309 ± 0.005 nC/Gy, respectively.

The results of the fD response linearity tests are reported in Figure 1. In Figure 1a, the DPP was varied by changing the applicator and keeping constant 4 μs pulse duration. An uncertainty of ±5% was associated with EBT-XD dose determination. Such a value was derived from repeatability tests and thus includes both the intrinsic uncertainty on the EBT-XD measurements as well as possible fluctuations of the accelerator output. The dashed red line is the linear best fit to the experimental data, with a slope of 0.306 ± 0.01 nC/Gy. In Figure 1b, the pulse duration was changed instead, from 1 up to 4 μs. In this case, the slope of the linear best fit is 0.310 ± 0.01 nC/Gy.

In Figure 2, the PDDs measured by the fD prototype and reference detectors are reported, both in conventional (Figure 2a) and UH-DPP (Figure 2b) modalities, in the case of the 100 mm applicator under 9 MeV energy beam irradiation. The depths corresponding to 90% and 50% of the maximum dose (R_{90} and R_{50}, respectively) were extracted from the PDD curves and summarized in Table 2. A maximum difference of about 0.5 mm is observed in the R_{90} and R_{50} values obtained from all the detectors in each modality.

Normalized beam profiles of two field sizes (FSs) (applicators 100 and 40 mm) are reported in Figure 3, both in conventional (a) and UH-DPP (b) modalities. In particular, the response of the fD prototype was compared with one of the SiD detector in Figure 3a, whereas in Figure 3b the results from EBT-XD films were used for comparison instead. The corresponding

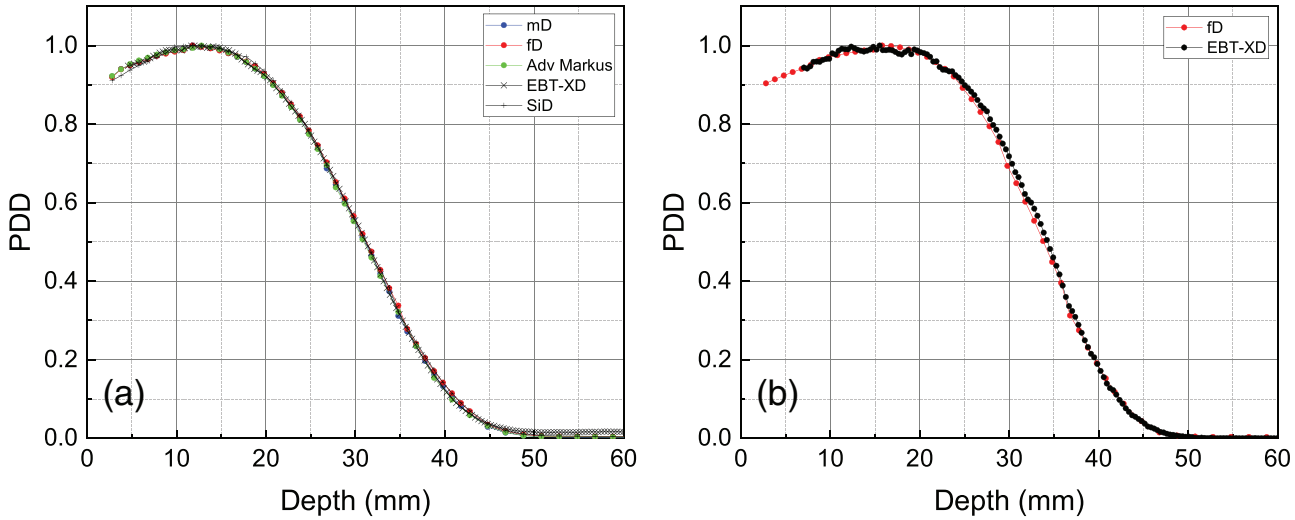

FIGURE 2 Percentage depth doses (PDDs) measured by the flashDiamond (fD) prototype and reference detectors in the case of the 100 mm PMMA applicator and 9 MeV beam energy, both in conventional (a) and ultrahigh-dose-per-pulse (UH-DPP) (b) modalities

TABLE 2 R_{90} and R_{50} of the 9 MeV beams in conventional and ultrahigh-dose-per-pulse (UH-DPP) modalities, calculated from the percentage depth dose (PDDs) measured with the 100m applicator by the flashDiamond (fD), microDiamond (mD), Advanced Markus, EBT-XD and silicon diode (SiD) detectors

	Conventional		UH-DPP	
Detector	R_{90}	R_{50}	R_{90}	R_{50}
fD	21.0	31.3	24.5	33.8
EBT-XD	20.9	31.2	25.0	34.3
mD	20.8	31.1		
SiD	21.2	31.2		
Adv. Markus	20.8	30.9		

Note: All data are expressed in mm.

values of average penumbra, FS, and profile flatness are summarized in Table 3. The latter was calculated as $100 \times (D_{max} - D_{min})/(D_{max} + D_{min})$, where D_{max} is the maximum dose measured in the central region corresponding to 80% of the FS, whereas D_{min} is the minimum dose over the same region. OFs are reported in Figure 4 and summarized in Table 4, as measured by using all the available PMMA applicators, beam energies, and irradiation modalities. Again, the fD response was compared with the one of the SiD detectors in conventional modality (Figure 4a) and EBT-XD films in UH-DPP modality (Figure 4b).

The commissioning of the ElectronFlash linac by the fD detector was completed by the acquisition of PDD and beam profile datasets at 9 and 7 MeV, by using all the applicators, in conventional and UH-DPP modalities. The obtained results are summarized in Table 5 (PDDs) and Table 6 (beam profiles). In Figures 5 and 6, PDDs and profiles are reported in the of UH-DPP modality only, more relevant for the aims of the present study.

4 | DISCUSSION

The aim of the present work is to test a novel diamond detector prototype as a tool for the commissioning of a linac capable of UH-DPP and UH-DR irradiation modalities. As such, the investigated detector was first calibrated in different facilities: at PTW under ^{60}Co irradiation, at PTB under UH-DPP electron beams, and at SIT under pulse electron beams in conventional modality. The values obtained under electron irradiation at SIT and PTB are in agreement, thus indicating that no differences are observed in the fD response when conventional and UH-DPP electron beams are used. In addition, the calibration coefficients obtained by ^{60}Co and electron beam irradiation are also in agreement within the experimental uncertainties. As a consequence, the beam quality correction factor from ^{60}Co to electron beams is unity within the experimental uncertainty. This is consistent with what is reported in the literature for the mD, in which case the deviation of the detector sensitivity under ^{60}Co and high energy electron beam irradiation was found to be lower than 0.5% by Monte Carlo simulations[37] and confirmed experimentally to be lower than 1%.[38]

The linearity tests, whose results are reported in Figure 1, demonstrate that the fD response is linear at least up to the maximum DPP of 11.9 Gy available in this study, well in the UH-DPP range. This confirms the results previously reported for fDs by the authors.[33] Two experimental data shown in Figure 1a and obtained by using the 30 and 35 mm applicators, that is, the

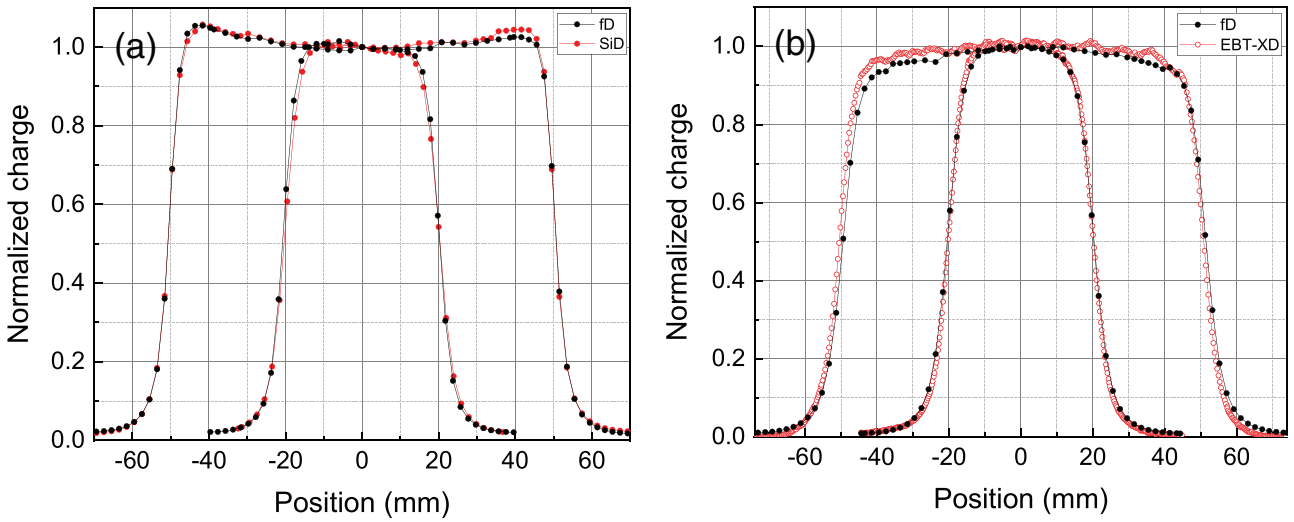

FIGURE 3 Beam profiles measured by the flashDiamond (fD) prototype and reference detectors in the case of the 100 and 40 mm PMMA applicators, 9 MeV beam energy, both in conventional (a) and ultrahigh-dose-per-pulse (UH-DPP) (b) modalities

TABLE 3 Average 80%–20% penumbra, field size (FS) and flatness of the 9 MeV conventional and ultrahigh-dose-per-pulse (UH-DPP) beams calculated from the profiles with 100 and 40 mm applicators measured by the flashDiamond (fD), silicon diode (SiD) and EBT-XD

Conventional						
	100 mm			**40 mm**		
Detector	**Penumbra (mm)**	**FS (mm)**	**Flatness (%)**	**Penumbra (mm)**	**FS (mm)**	**Flatness (%)**
fD	4.7	101.5	3.0	5.1	41.1	5.2
SiD	4.7	101.4	2.8	5.8	40.7	6.9
UH-DPP						
	100 mm			**40 mm**		
Detector	**Penumbra (mm)**	**FS (mm)**	**Flatness (%)**	**Penumbra (mm)**	**FS (mm)**	**Flatness (%)**
fD	7.2	101.0	3.4	6.7	40.9	8.8
EBT-XD	6.5	101.3	3.4	6.0	40.5	7.6

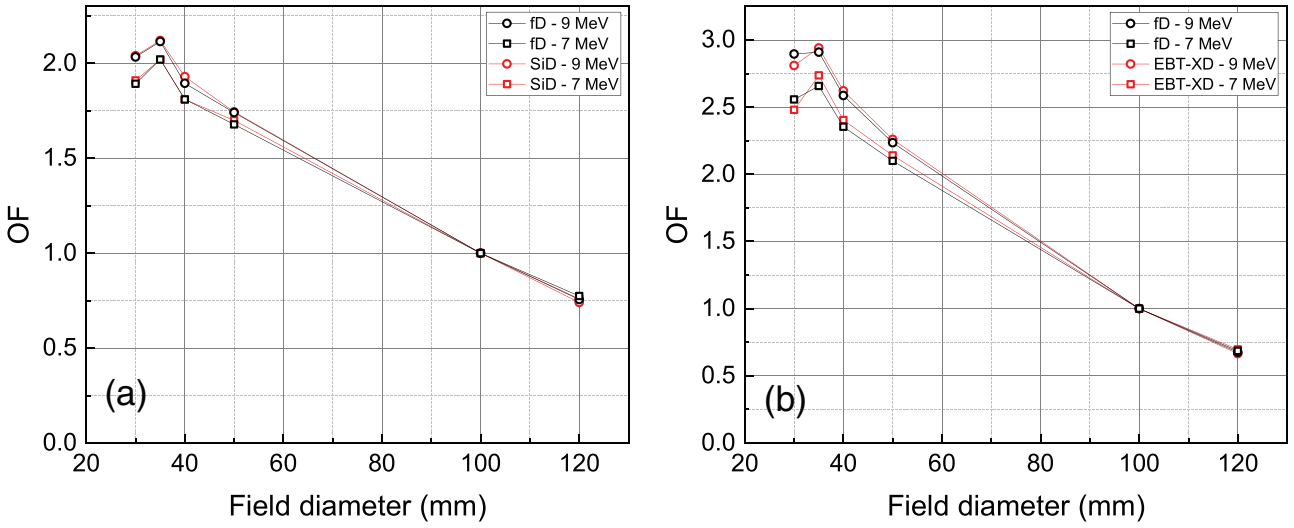

FIGURE 4 Output factors (OFs) measured by the flashDiamond (fD) prototype and reference detectors by using all the applicators and the beam energies, both in conventional (a) and ultrahigh-dose-per-pulse (UH-DPP) (b) modalities

TABLE 4 Output factors (OFs) measured by the flashDiamond (fD) prototype and reference detectors by using all the applicators and the beam energies, both in conventional and ultrahigh-dose-per-pulse (UH-DPP) modalities

	Conventional				UH-DPP			
	7 MeV		9 MeV		7 MeV		9 MeV	
Ø (mm)	fD	SiD	fD	SiD	fD	EBT-XD	fD	EBT-XD
30	1.89	1.91	2.03	2.04	2.56	2.48	2.90	2.81
35	2.02	2.02	2.11	2.12	2.66	2.74	2.91	2.94
40	1.81	1.81	1.89	1.93	2.35	2.40	2.59	2.62
50	1.68	1.70	1.74	1.74	2.10	2.14	2.23	2.26
100	1.00	1.00	1.00	1.00	1.00	1.00	1.00	1.00
120	0.77	0.76	0.76	0.74	0.68	0.70	0.67	0.66

TABLE 5 R_{90} and R_{50} of the 7 and 9 MeV conventional and ultrahigh-dose-per-pulse (UH-DPP) beams extracted from the percentage depth dose (PDDs) measured by the flashDiamond (fD) with different applicators

	7 MeV				9 MeV			
	Conventional		UH-DPP		Conventional		UH-DPP	
Ø	R_{90}	R_{50}	R_{90}	R_{50}	R_{90}	R_{50}	R_{90}	R_{50}
30	15.9	23.7	18.7	26.0	20.2	29.9	23.1	32.9
35	16.9	24.7	18.2	25.4	21.4	31.2	24.1	33.3
40	17.1	24.7	19.2	26.2	21.9	31.5	25.1	34.3
50	17.3	25.0	18.3	25.5	22.5	31.9	25.1	33.9
100	15.7	23.8	17.8	24.9	21.0	31.3	24.5	33.8
120	14.8	23.0	17.3	24.7	19.5	30.0	24.2	33.4

Note: All data are expressed in mm.

TABLE 6 Average values of the 80%–20% penumbras, field sizes (FSs), and flatness of the 7 and 9 MeV conventional and ultrahigh-dose-per-pulse (UH-DPP) beams calculated from the profiles measured by the flashDiamond (fD) using applicators of different diameters

	7 MeV						9 MeV					
	Conventional			UH-DPP			Conventional			UH-DPP		
Ø (mm)	Penumbra (mm)	FS (mm)	Flatness (%)	Penumbra (mm)	FS (mm)	Flatness (%)	Penumbra (mm)	FS (mm)	Flatness (%)	Penumbra (mm)	FS (mm)	Flatness (%)
30	5.4	30.9	9.5	6.0	30.8	11.6	4.8	31.2	7.9	6.1	31.2	10.7
35	5.2	37.2	6.2	5.8	37.0	8.9	5.2	37.5	5.8	6.5	37.3	9.1
40	5.2	40.8	5.8	5.9	40.5	7.6	5.1	41.1	5.2	6.7	40.9	8.6
50	5.0	51.2	2.8	4.6	51.2	2.8	5.7	51.5	3.6	7.3	51.4	7.4
100	4.3	101.2	2.3	5.3	101.0	1.1	4.7	101.5	3.0	7.2	101.0	3.4
120	4.0	126.8	2.2	5.3	126.6	1.7	4.5	127.2	2.9	7.6	126.4	3.8

ones at the highest DPPs in the plot, deserve a specific comment. Very similar charges, and thus DPPs are measured by the fD detector. This is not the case for the EBT-XD values, the DPP acquired with the 35 mm applicator being about 4% higher (see Table 1). Indeed, according to the 5% uncertainty associated with the EBT-XD dose measurements, such two values can be considered consistent within the experimental error.

The detector sensitivities were derived from the slopes of the linear best fits, both in Figure 1a and 1b. The obtained values of 0.306 ± 0.01 nC/Gy (Figure 1a) and 0.310 ± 0.01 nC/Gy (Figure 1b) are consistent with the previously reported calibration coefficients, thus providing a further cross-calibration of the fD detector against the reference EBT-XD films. However, a higher uncertainty is associated with such sensitivities, basically due to the relatively poor accuracy of the EBT-XD dose determination.

The next step in the dosimetric validation of the fD prototype was the comparison of its response with the

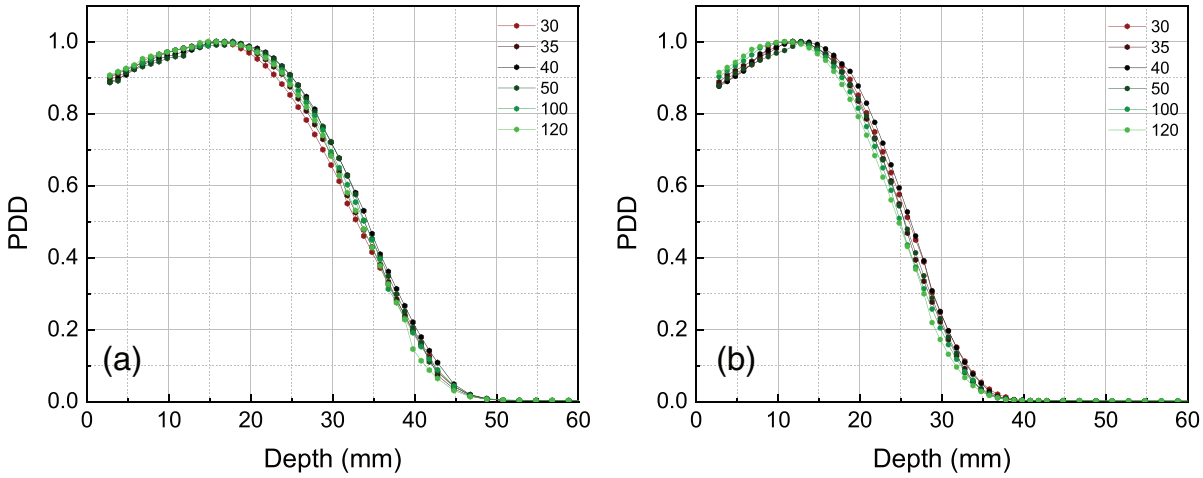

FIGURE 5 Percentage depth dose (PDDs) measured by the flashDiamond (fD) prototype irradiated in ultrahigh-dose-per-pulse (UH-DPP) modality, by using all the applicators and beam energies, in the case of 9 MeV (a) and 7 MeV (b)

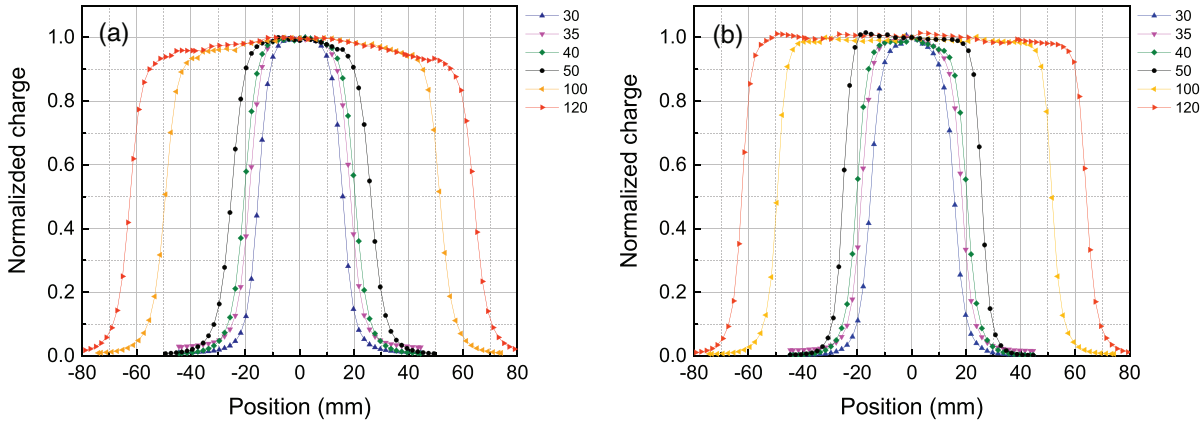

FIGURE 6 Beam profiles measured by the flashDiamond (fD) prototype irradiated in ultrahigh-dose-per-pulse (UH-DPP) modality, by using all the applicators and beam energies, in the case of 9 MeV (a) and 7 MeV (b)

ones obtained by well-assessed reference detectors, in terms of PDD and profile curve measurements. As for the PDDs, Figure 2 and Table 2 demonstrate a general very good agreement. In particular, according to the experimental datasets reported in Figure 2a for conventional beam modality, an agreement is observed within 0.3 mm among the R_{50} values obtained by using the five detectors, namely fD, mD, SiD, Advanced Markus, and EBT-XD, which is compatible with the estimated positioning error. A small overestimation of about 1% is indeed observed in the case of EBT-XD with respect to all the other detectors at depths exceeding about 45 mm, where very low doses are measured, below the EBT-XD dynamic range recommended by the manufacturer. In Figure 2b the PDD curves are reported for UH-DPP irradiation conditions. In this case, the fD prototype response could be compared with the one from EBT-XD films only, all other detectors being unsuitable for measuring such high DPPs. A good agreement is confirmed between the two PDDs with a difference of the R_{50} values of about 0.5 mm, even though a somewhat noisier curve is observed from the films. The results obtained both by the calibration procedures and the PDD measurements demonstrate that the fD response is independent from the beam energies used in the present study.

The beam profile curves acquired by the fD prototypes were compared with the ones obtained by an SiD detector in the case of conventional irradiation modality, and EBT-XD films in UH-DPP conditions. The results are summarized in Figure 3 and Table 3. An overall good agreement is again observed between the fD curves, and those from the reference detectors. Just as for the PDD measurements, noisier curves are obtained from EBT-XD films and small deviations can be noticed in the out-of-field low dose regions. As far as the penumbras are concerned, the values reported in Table 3 are in good agreement, showing a maximum difference of

0.7 mm. As the active area diameters of the fD and SiD detectors are 1.4 and 1.2 mm,[39,40] respectively, both smaller than the intrinsic penumbra of the 100 and 40 mm beam sizes, the observed discrepancies are likely ascribed to the measurement uncertainty rather than to a different spatial resolution of the three detectors.

OFs were then measured by using the fD detector and compared with the ones of the SiD in the case of conventional irradiation modality and with the EBT-XD responses in UH-DPP conditions. All the fD OFs are in agreement with those measured by reference detectors. However, it is noticed that larger discrepancies are observed in the comparison with EBT-XD film values, up to a maximum value of about 3%. Again, this is consistent with the 5% uncertainty associated with the GAFchromic film dose determination.

After the previously reported fD detector prototype characterization, the focus of the present study was addressed to the completion of the ElectronFlash commissioning procedure. To this purpose, PDDs and beam profiles were acquired for all the available beam energies, irradiation modalities, and PMMA applicators. The fD detector position was manipulated in a PTW motorized water phantom in combination with the Mephysto MC^2 software. The obtained results are summarized in Tables 5 and 6, and specifically reported in Figures 5 and 6 for the case of UH-DPP modality only. As for the PDD curves, it is worth mentioning that the combination of applicator lengths and diameters results in a different contribution from scattered electrons, and thus to the small differences in the R_{50} values reported in Table 5 and noticeable in Figure 5. As far as the beam profiles are concerned, a somewhat higher out-of-field dose values can be appreciated in Figure 6 in the case of the 35 mm applicator. This is ascribed to the smaller wall thickness (2 mm instead of 5 mm, see Table 1) of this specific applicator, allowing for a larger number of electrons escaping the applicator and contributing to the overall dose in the out-of-field region.

5 | CONCLUSIONS

A detailed dosimetric characterization of an fD detector prototype was carried out, in terms of absolute dose, response linearity, PDDs, beam profiles, and OF determinations. To this purpose, an ElectronFlash linac was used, operated both in conventional and UH-DPP irradiation modalities, covering a DPP range up to 11.9 Gy. Several well-assessed commercial dosimeters were used for comparison, in measurements performed in both irradiation conditions. The results obtained from the previously reported comprehensive characterization provide an experimental validation of the fD prototype from the dosimetric point of view and demonstrate its suitability as a valuable tool for the commissioning of FLASH-RT electron beam linacs. Monte Carlo simulations of both the ElectronFlash linac beams and the fD detector are in progress as well, in order to provide theoretical support to the dosimetric validation reported in this study.

ACKNOWLEDGMENTS

The present work is part of the 18HLT04 UHDpulse project (http://uhdpulse-empir.eu/), which has received funding from the European Metrology Programme for Innovation and Research (EMPIR) program, cofinanced by the Participating States and from the European Union's Horizon 2020 research and innovation program. We wish to thank PTW-Freiburg for cooperation in the diamond prototype production and Thomas Hackel for the assistance in the fD calibration at PTB.

CONFLICT OF INTEREST

Marco Marinelli and Gianluca Verona Rinati signed a contract with PTW-Freiburg involving financial interests deriving from the PTW microDiamond 60019 dosimeter commercialization. Giuseppe Felici is an SIT S.p.A. shareholder. Matteo Pacitti and Federica Galante are SIT S.p.A. employees. Rafael Kranzer is a PTW-Freiburg employee. Alessia Gasparini received a grant for a postdoc position funded by SIT S.p.A.

REFERENCES

1. Favaudon V, Caplier L, Monceau V, et al. Ultrahigh dose-rate FLASH irradiation increases the differential response between normal and tumor tissue in mice. *Sci Transl Med*. 2014;6(245):245ra93-245ra93. https://doi.org/10.1126/scitranslmed.3008973
2. Fouillade C, Favaudon V, Vozenin MC, et al. Les promesses du haut débit de dose en radiothérapie. *Bull Cancer*. 2017;104(4):380-384. https://doi.org/10.1016/j.bulcan.2017.01.012
3. Montay-Gruel P, Petersson K, Jaccard M, et al. Irradiation in a flash: unique sparing of memory in mice after whole brain irradiation with dose rates above 100 Gy/s. *Radiother Oncol*. 2017;124(3):365-369. https://doi.org/10.1016/j.radonc.2017.05.003
4. Durante M, Brauer-Krisch E, Hill M. Faster and safer? FLASH ultra-high dose rate in radiotherapy. *Br J Radiol*. 2017;91:20170628. https://doi.org/10.1259/bjr.20170628. Published online November 27
5. Bourhis J, Montay-Gruel P, Gonçalves Jorge P, et al. Clinical translation of FLASH radiotherapy: why and how?. *Radiother Oncol*. 2019;139:11-17. https://doi.org/10.1016/j.radonc.2019.04.008
6. Vozenin MC, Hendry JH, Limoli CL. Biological benefits of ultra-high dose rate FLASH radiotherapy: sleeping beauty awoken. *Clin Oncol*. 2019;31(7):407-415. https://doi.org/10.1016/j.clon.2019.04.001
7. Vozenin MC, Baumann M, Coppes RP, Bourhis J. FLASH radiotherapy International workshop. *Radiother Oncol*. 2019;139:1-3. https://doi.org/10.1016/j.radonc.2019.07.020
8. Esplen N, Mendonca MS, Bazalova-Carter M. Physics and biology of ultrahigh dose-rate (FLASH) radiotherapy: a topical review. *Phys Med Biol*. 2020;65(23):23TR03. https://doi.org/10.1088/1361-6560/abaa28
9. Schüller A, Heinrich S, Fouillade C, et al. The European joint research project UHDpulse – metrology for advanced radiotherapy using particle beams with ultra-high pulse dose rates. *Physica Med*. 2020;80:134-150. https://doi.org/10.1016/j.ejmp.2020.09.020

10. Wilson JD, Hammond EM, Higgins GS, Petersson K. Ultra-high dose rate (FLASH) radiotherapy: silver bullet or fool's gold?. *Front Oncol*. 2020;9:1563. https://doi.org/10.3389/fonc.2019.01563
11. Marcu LG, Bezak E, Peukert DD, Wilson P. Translational research in FLASH radiotherapy—from radiobiological mechanisms to in vivo results. *Biomedicines*. 2021;9(2):181. https://doi.org/10.3390/biomedicines9020181
12. Lin B, Gao F, Yang Y, et al. FLASH radiotherapy: history and future. *Front Oncol*. 2021;11:644400. https://doi.org/10.3389/fonc.2021.644400
13. Schüler E, Trovati S, King G, et al. Experimental platform for ultra-high dose rate FLASH irradiation of small animals using a clinical linear accelerator. *Int J Radiat Oncol Biol Phys*. 2017;97(1):195-203. https://doi.org/10.1016/j.ijrobp.2016.09.018
14. Patriarca A, Fouillade C, Auger M, et al. Experimental set-up for FLASH proton irradiation of small animals using a clinical system. *Int J Radiat Oncol Biol Phys*. 2018;102(3):619-626. https://doi.org/10.1016/j.ijrobp.2018.06.403
15. Di Martino F, Barca P, Barone S, et al. FLASH radiotherapy with electrons: issues related to the production, monitoring, and dosimetric characterization of the beam. *Front Phys*. 2020;8:570697. https://doi.org/10.3389/fphy.2020.570697
16. Jaccard M, Durán MT, Petersson K, et al. High dose-per-pulse electron beam dosimetry: commissioning of the Oriatron eRT6 prototype linear accelerator for preclinical use. *Med Phys*. 2018;45(2):863-874. https://doi.org/10.1002/mp.12713
17. Lansonneur P, Favaudon V, Heinrich S, Fouillade C, Verrelle P, De Marzi L. Simulation and experimental validation of a prototype electron beam linear accelerator for preclinical studies. *Physica Med*. 2019;60:50-57. https://doi.org/10.1016/j.ejmp.2019.03.016
18. Faillace L, Barone S, Battistoni G, et al. Compact S-band linear accelerator system for ultrafast, ultrahigh dose-rate radiotherapy. *Phys Rev Accel Beams*. 2021;24(5):050102. https://doi.org/10.1103/PhysRevAccelBeams.24.050102
19. Moeckli R, Gonçalves Jorge P, Grilj V, et al. Commissioning of an ultra-high dose rate pulsed electron beam medical LINAC for FLASH RT preclinical animal experiments and future clinical human protocols. *Med Phys*. 2021;48(6):3134-3142. https://doi.org/10.1002/mp.14885
20. Ashraf MR, Rahman M, Zhang R, et al. Dosimetry for FLASH radiotherapy: a review of tools and the role of radioluminescence and Cherenkov emission. *Front Phys*. 2020;8:328. https://doi.org/10.3389/fphy.2020.00328
21. Kokurewicz K, Schüller A, Brunetti E, et al. Dosimetry for new radiation therapy approaches using high energy electron accelerators. *Front Phys*. 2020;8:568302. https://doi.org/10.3389/fphy.2020.568302
22. Bourhis J, Sozzi WJ, Jorge PG, et al. Treatment of a first patient with FLASH-radiotherapy. *Radiother Oncol*. 2019;139:18-22. https://doi.org/10.1016/j.radonc.2019.06.019
23. Vozenin MC, De Fornel P, Petersson K, et al. The advantage of FLASH radiotherapy confirmed in mini-pig and cat-cancer patients. *Clin Cancer Res*. 2019;25(1):35-42. https://doi.org/10.1158/1078-0432.CCR-17-3375
24. Kranzer R, Poppinga D, Weidner J, et al. Ion collection efficiency of ionization chambers in ultra-high dose-per-pulse electron beams. *Med Phys*. 2021;48(2):819-830. https://doi.org/10.1002/mp.14620
25. Gondré M, Jorge PG, Vozenin MC, et al. Optimization of alanine measurements for fast and accurate dosimetry in FLASH radiation therapy. *Radiat Res*. 2020;194(6):573-579. https://doi.org/10.1667/RR15568.1
26. Jorge PG, Jaccard M, Petersson K, et al. Dosimetric and preparation procedures for irradiating biological models with pulsed electron beam at ultra-high dose-rate. *Radiother Oncol*. 2019;139:34-39. https://doi.org/10.1016/j.radonc.2019.05.004
27. Lempart M, Blad B, Adrian G, et al. Modifying a clinical linear accelerator for delivery of ultra-high dose rate irradiation. *Radiother Oncol*. 2019;139:40-45. https://doi.org/10.1016/j.radonc.2019.01.031
28. Jaccard M, Petersson K, Buchillier T, et al. High dose-per-pulse electron beam dosimetry: usability and dose-rate independence of EBT3 Gafchromic films. *Med Phys*. 2017;44(2):725-735. https://doi.org/10.1002/mp.12066
29. Petersson K, Jaccard M, Germond JF, et al. High dose-per-pulse electron beam dosimetry – a model to correct for the ion recombination in the Advanced Markus ionization chamber. *Med Phys*. 2017;44(3):1157-1167. https://doi.org/10.1002/mp.12111
30. McManus M, Romano F, Lee ND, et al. The challenge of ionisation chamber dosimetry in ultra-short pulsed high dose-rate very high energy electron beams. *Sci Rep*. 2020;10(1):9089. https://doi.org/10.1038/s41598-020-65819-y
31. Vignati A, Giordanengo S, Fausti F, et al. Beam monitors for tomorrow: the challenges of electron and photon FLASH RT. *Front Phys*. 2020;8:375. https://doi.org/10.3389/fphy.2020.00375
32. Bourgouin A, Schüller A, Hackel T, et al. Calorimeter for real-time dosimetry of pulsed ultra-high dose rate electron beams. *Front Phys*. 2020;8:567340. https://doi.org/10.3389/fphy.2020.567340
33. Marinelli M, Felici G, Galante F, et al. Design, realization, and characterization of a novel diamond detector prototype for FLASH radiotherapy dosimetry. *Med Phys*. 2022:49:1902-1910. https://doi.org/10.1002/mp.15473. In press
34. International Electrotechnical Commission 2020 Medical electrical equipment – Part 2-1: Particular requirements for the basic safety and essential performance of electron accelerators in the range 1 MeV to 50 MeV IEC 60601-2-1:2020 232. https://webstore.iec.ch/publication/31388
35. Almaviva S, Marinelli M, Milani E, et al. Chemical vapor deposition diamond based multilayered radiation detector: physical analysis of detection properties. *J App Phys*. 2010;107(1):014511. https://doi.org/10.1063/1.3275501
36. Marinelli M, Prestopino G, Verona C, Verona-Rinati G. Experimental determination of the PTW 60019 microDiamond dosimeter active area and volume. *Med Phys*. 2016;43(9):5205-5212. https://doi.org/10.1118/1.4961402
37. Pimpinella M, Stravato A, Guerra AS, Marinelli M, Verona-Rinati G. Monte Carlo calculation of beam quality correction factors for the PTW microDiamond in high energy photon and electron beams. *Physica Med*. 2015;31:e53. https://doi.org/10.1016/j.ejmp.2015.10.083
38. Di Venanzio C, Marinelli M, Tonnetti A, et al. Characterization of a microDiamond detector in high-dose-per-pulse electron beams for intra operative radiation therapy. *Physica Med*. 2015;31(8):897-902. https://doi.org/10.1016/j.ejmp.2015.06.008
39. Schönfeld AB, Poppinga D, Kranzer R, et al. Technical note: Characterization of the new microSilicon diode detector. *Med Phys*. 2019;46(9):4257-4262. https://doi.org/10.1002/mp.13710
40. Poppinga D, Kranzer R, Ulrichs A, et al. Three-dimensional characterization of the active volumes of PTW microDiamond, microSilicon, and Diode E dosimetry detectors using a proton microbeam. *Med Phys*. 2019;46(9):4241-4245. https://doi.org/10.1002/mp.13705

How to cite this article: Verona Rinati G, Felici G, Galante F, et al. Application of a novel diamond detector for commissioning of FLASH radiotherapy electron beams. *Med Phys*. 2022;1-10. https://doi.org/10.1002/mp.15782